

Universität des Saarlandes



Fachrichtung 6.1 – Mathematik

Preprint Nr. 153

**A Shock-Capturing Algorithm for the
Differential Equations of Dilation and Erosion**

Michael Breuß and Joachim Weickert

Saarbrücken 2005

A Shock-Capturing Algorithm for the Differential Equations of Dilation and Erosion

Michael Breuß

Technical University Brunswick
Computational Mathematics
Pockelsstraße 14
38106 Brunswick, Germany
`m.breuss@tu-bs.de`

Joachim Weickert

Mathematical Image Analysis Group
Faculty of Mathematics and Computer Science
Saarland University
66041 Saarbrücken, Germany
`weickert@mia.uni-saarland.de`

Edited by
FR 6.1 – Mathematik
Universität des Saarlandes
Postfach 15 11 50
66041 Saarbrücken
Germany

Fax: + 49 681 302 4443
e-Mail: preprint@math.uni-sb.de
WWW: <http://www.math.uni-sb.de/>

Abstract

Dilation and erosion are the fundamental operations in morphological image processing. Algorithms that exploit the formulation of these processes in terms of partial differential equations offer advantages for non-digitally scalable structuring elements and allow sub-pixel accuracy. However, the widely-used schemes from the literature suffer from significant blurring at discontinuities. We address this problem by developing a novel, flux corrected transport (FCT) type algorithm for morphological dilation / erosion with a flat disc. It uses the viscosity form of an upwind scheme in order to quantify the undesired diffusive effects. In a subsequent corrector step we compensate for these artifacts by means of a stabilised inverse diffusion process that requires a specific nonlinear multidimensional formulation. We prove a discrete maximum–minimum principle in this multidimensional framework. Our experiments show that the method gives a very sharp resolution of moving fronts, and it approximates rotation invariance very well.

Key Words: morphological dilation, morphological erosion, finite difference methods, flux corrected transport

AMS Classification: 35L60, 65M06, 65M12, 68U10

1 Introduction

Mathematical morphology is concerned with image analysis of shapes. It is one of the oldest and most successful areas of digital image processing; see e.g. the textbooks [10, 15, 21, 27, 28, 29, 34] and the proceedings volumes [14, 16, 20, 24, 30, 31, 36] for an overview. Its fundamental operations are called *dilation* and *erosion*. For some greyscale image $f : \mathbb{R}^2 \rightarrow \mathbb{R}$ and a so-called structuring element $B \subset \mathbb{R}^2$, dilation and erosion are defined by

$$\text{dilation:} \quad (f \oplus B)(\mathbf{x}) := \sup \{f(\mathbf{x}-\mathbf{z}), \mathbf{z} \in B\}, \quad (1)$$

$$\text{erosion:} \quad (f \ominus B)(\mathbf{x}) := \inf \{f(\mathbf{x}+\mathbf{z}), \mathbf{z} \in B\}. \quad (2)$$

They form the basis of many other morphological processes such as openings, closings, top hats and morphological derivative operators.

While dilation and erosion are frequently implemented by algebraic set operations, for convex structuring elements there is also an alternative formulation in terms of partial differential equations (PDEs) [1, 2, 7, 37]. Let us consider a convex structuring element tB with a scaling parameter $t > 0$. Then, it can

be shown that the calculation of $u(\mathbf{x}, t) = f \oplus tB$ and $u(\mathbf{x}, t) = f \ominus tB$ is equivalent to solving the PDEs

$$\partial_t u(\mathbf{x}, t) = \sup_{\mathbf{z} \in B} \langle \mathbf{z}, \nabla u(\mathbf{x}, t) \rangle, \quad (3)$$

$$\partial_t u(\mathbf{x}, t) = \inf_{\mathbf{z} \in B} \langle \mathbf{z}, \nabla u(\mathbf{x}, t) \rangle, \quad (4)$$

with f as initial condition [1, 26], respectively. Here, $\nabla = (\partial_x, \partial_y)^\top$ denotes the spatial nabla operator, and $\langle \cdot, \cdot \rangle$ is the Euclidean inner product. By choosing, e.g., a disc

$$B := \{ \mathbf{z} \in \mathbb{R}^2, \|\mathbf{z}\|_2 \leq 1 \},$$

one obtains

$$\text{dilation:} \quad \partial_t u = \|\nabla u\|_2, \quad (5)$$

$$\text{erosion:} \quad \partial_t u = -\|\nabla u\|_2. \quad (6)$$

The solution at “time” t is the dilation (resp. erosion) of f with a disc of radius t and center 0 as structuring element.

The dilation/erosion PDEs (5)–(6) belong to the class of so-called *hyperbolic* PDEs, see e.g. [11, 12] to learn more about partial differential equations. Hyperbolic processes describe evolutions that propagate information with finite speed, similar as wave propagation. They may create shocks even if the initial data are smooth, and they require specific numerical schemes that take into account the propagation direction and handle shock-like discontinuities in a graceful manner [19]. Since many hyperbolic PDEs arise in computational fluid dynamics, it is natural to derive numerical methods for the dilation/erosion equations from techniques for hyperbolic conservation laws. In particular, finite difference methods such as the *Osher–Sethian schemes* [22, 23, 32] and the *Rouy–Tourin method* [25, 38] are widely-used in this context.

PDE-based algorithms for dilation/erosion offer two advantages over classical set-theoretic schemes [2, 8, 26]: first of all, they give excellent results for non-digitally scalable structuring elements whose shapes cannot be represented correctly on a discrete grid, for instance discs or ellipses. Secondly, the time t plays the role of a continuous scale parameter. Therefore, the size of a structuring element does not need to be multiples of the pixel size, and it is possible to get results with sub-pixel accuracy.

On the other hand, the main disadvantage of typical PDE-based algorithms for mathematical morphology consists of the fact that dissipative effects such as blurring of discontinuities occur. Apart from an investigation on the use-

fulness of high-order ENO¹ schemes [33, 35], we are not aware of attempts in the literature to deal with these undesired *numerical diffusion* artifacts in PDE schemes for mathematical morphology.

It is the goal of the present paper to address this problem. For the development of our algorithm, we focus on the dilation process (5) since the erosion process can be treated analogously. We develop a new variant of the *flux corrected transport (FCT)* technique of Boris and Book [3, 4, 5, 17, 40] introduced in the context of fluid flow simulation. Our FCT scheme is used for approximating one- and two-dimensional morphological processes in an *accurate* and *rotationally invariant* fashion. The aim of this paper is especially to give a detailed derivation and a sound mathematical basis for the 1-D and 2-D algorithms.

Related Work. The general idea behind the FCT technique is to compute in a first step the evolution with a scheme that may incorporate much numerical diffusion. Afterwards, this diffusion is annihilated in a proper fashion by applying a *stabilised inverse diffusion* step, sometimes also named *antidiffusion*. In conventional FCT methods, see especially [5], the amount of antidiffusion which is to be applied is basically determined by means of the so-called *modified equation* of the diffusive basis methods, see for instance [13, 19] for details concerning this notion. In some newer works mainly concerned with finite element schemes, antidiffusive fluxes are computed by *algebraic* properties of the entries of corresponding stiffness matrices, see e.g. [18] and the references therein. We employ a different approach motivated by the theory of numerical methods for conservation laws, compare e.g. [13]: we construct our FCT scheme considering the *viscosity form* of the underlying method. By the use of this form we can effectively eliminate the influence of the numerical viscosity due to the spatial derivative. It turns out that our scheme provides a much sharper resolution in comparison with the second-order high-resolution scheme of Osher and Sethian [23]. Let us note that in contrast to the classical works of Boris, Book and their collaborators, we derive the essential information for our algorithms on the *discrete* basis, while compared to the approach of Kuzmin and Turek [18] our proceeding is technically relatively simple.

Furthermore, both mentioned FCT approaches rely on an underlying *additive splitting* of the backward diffusion into fluxes between computational nodes: especially in the multidimensional case, the mentioned works proceed along the considerations of Zalesak [39]. In contrast, our *genuinely multidimensional*

¹ENO means *essentially non-oscillatory*. By adapting the stencil for derivative approximations to the local smoothness of the solution, ENO schemes obtain both high-order accuracy in smooth regions and sharp shock transitions.

mensional approach yielding directly the desired rotational invariance uses the dimensional dependent nonlinear form of the numerical viscosity. This proceeding is to our knowledge not explored up to now within the literature. However, its usefulness and simplicity is immediately evident in the image processing context presented here.

The algorithm we develop in our paper is close in spirit to a recent conference contribution by us, where we developed a FCT approach for three one-dimensional model equations for numerical conservation laws [6]. However, it should be noted that the dilation/erosion PDEs were are investigating in our present paper cannot be written in conservation form, and that we do not restrict ourselves to the 1-D case.

Organisation of the Paper. Our paper is organised as follows. In the next section we review some existing numerical schemes for PDE-based mathematical morphology. In Section 3 we introduce our novel FCT scheme for the dilation process in the 1-D case, where we describe the upwind scheme as predictor, and introduce an inverse diffusion algorithm as corrector. We illustrate its behaviour by an experiment and establish stability results in terms of a maximum principle. Section 4 extends these investigations to the 2-D case. The paper is concluded with a summary in Section 5.

2 Existing Algorithms

As already mentioned, prominent PDE-based algorithms for the dilation equation are the and the first- and second-order methods of Osher and Sethian [22, 23, 32], and the first-order scheme of Rouy and Tourin [25, 38]. For the dilation equation

$$\partial_t u = \|\nabla u\|_2 = ((\partial_x u)^2 + (\partial_y u)^2)^{1/2} \quad (7)$$

the Rouy–Tourin scheme is given by

$$U_{i,j}^{n+1} = U_{i,j}^n + \lambda \left(\left(\max(0, U_{i+1,j}^n - U_{i,j}^n, U_{i-1,j}^n - U_{i,j}^n) \right)^2 + \left(\max(0, U_{i,j+1}^n - U_{i,j}^n, U_{i,j-1}^n - U_{i,j}^n) \right)^2 \right)^{1/2}, \quad (8)$$

and the first-order Osher–Sethian upwind scheme can be written as

$$U_{i,j}^{n+1} = U_{i,j}^n + \lambda \left(\left(\max(0, U_{i+1,j}^n - U_{i,j}^n) \right)^2 + \left(\max(0, U_{i-1,j}^n - U_{i,j}^n) \right)^2 + \left(\max(0, U_{i,j+1}^n - U_{i,j}^n) \right)^2 + \left(\max(0, U_{i,j-1}^n - U_{i,j}^n) \right)^2 \right)^{1/2}. \quad (9)$$

Thereby, we use as in the following the notation U for discrete data in contrast to the analytical solution u , and we denote the ratio of mesh sizes Δt and Δx in t and x direction by $\lambda = \Delta t / \Delta x$. We assume that $\Delta x = \Delta y$. The upper index k in $U_{l,m}^k$ denotes as usual the temporal level $k\Delta t$ while, analogously, the lower indices l and m specify the spatial mesh point $(l\Delta x, m\Delta y)$.

As indicated, the mentioned work of Osher and Sethian does not only deal with first-order upwinding, it also allows high-order approximations in the style of high-resolution slope-limiting TVD schemes for conservation laws: for the integration of fluxes accross cell boundaries, the discrete derivatives of grey values are corrected by a contribution taking into account the local discrete second order derivatives. We refrain from displaying the more complicated formulae here.

We test the mentioned approaches with a scenario that is sensitive to failures in the rotational invariance of a method, namely the dilation of a disc. Figure 1(a) shows the initial value of the dilation process. The circle is supposed to grow in a uniform fashion while the circular shape is preserved. In Figure 1(b) we see the initial image evolved by the Rouy–Tourin algorithm yielding a rotationally invariant, but somewhat blurred solution. In Figures 1(c) and (d), we illustrate the behaviour of the first-order Osher–Sethian upwind scheme and the second-order scheme, respectively, using for time integration as proposed in [23] the method of Heun. While both methods seem to approximate rotational invariance well, we also see that the Osher–Sethian approach with higher-order resolution does not yield a substantial increase in accuracy. Only within the details one observes a slightly better preservation of the circular shape while the circular front is a bit less smeared. This example demonstrates the need for alternative schemes with a better shock-capturing behaviour.

3 The One-Dimensional FCT Algorithm

We start our one-dimensional investigations in this section with a review of the essential properties of an upwind scheme for a general hyperbolic first-order PDE. Afterwards, we derive its specific structure for the case of a dilation equation and identify it with the Rouy–Tourin scheme. This scheme serves as first step in our FCT algorithm. In a second step we construct a suitable inverse diffusion step in order to compensate for the numerical viscosity that has been introduced by the upwind scheme. Finally we prove a discrete maximum principle for the FCT scheme.

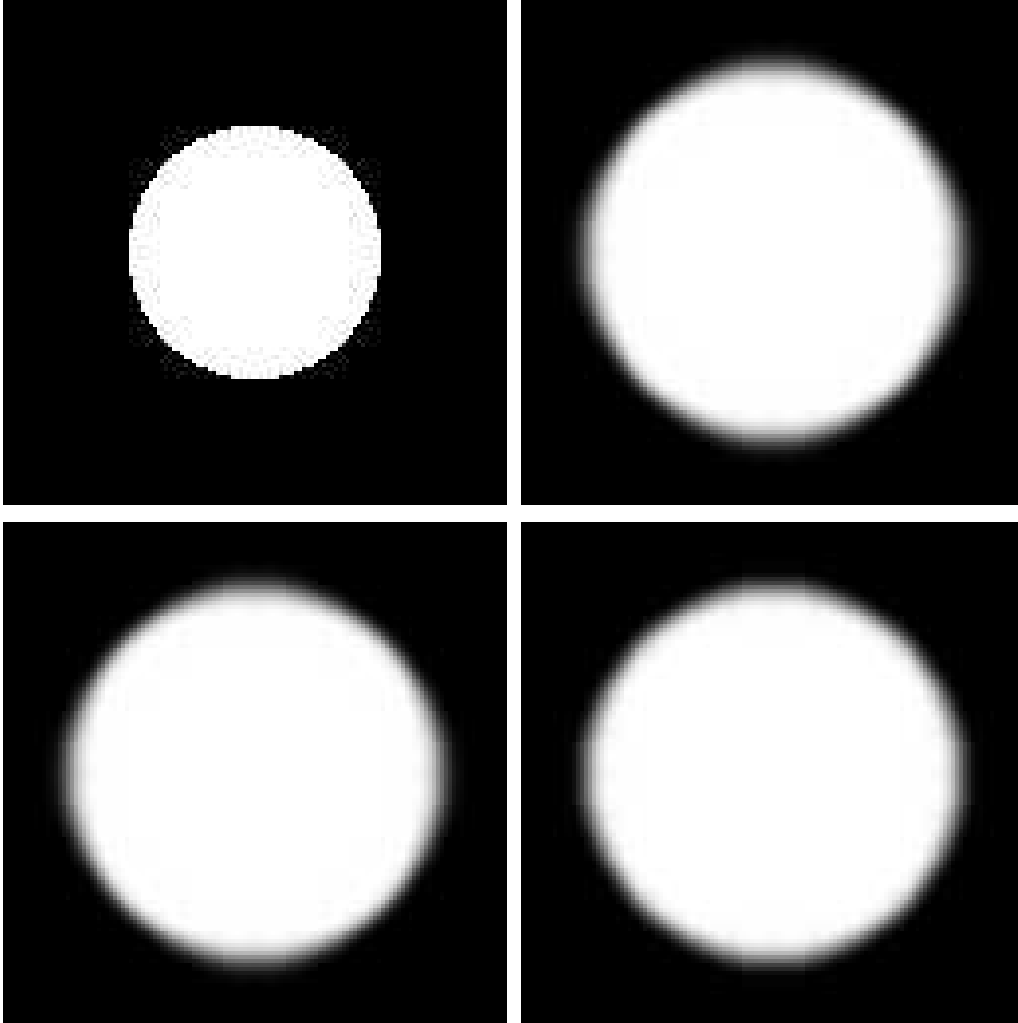


Figure 1: **(a) Top left:** Initial image, 128×128 pixels. **(b) Top right:** Image dilated by the Rouy–Tourin scheme ($\Delta x = \Delta y = 1$, $\Delta t = 0.5$, 30 iterations). **(c) Bottom left:** Dilated by the first-order upwind scheme (same parameters). **(d) Bottom right:** Dilated by a second-order Osher–Sethian scheme (same parameters).

3.1 The General Upwind Scheme in 1-D

The underlying method for our new FCT technique is the classical *upwind scheme*. For a general one-dimensional hyperbolic first-order PDE $u_t + (f(u))_x = 0$ with $f'(\cdot) \geq 0$ it can be written as

$$U_j^{n+1} = U_j^n - \lambda \left(f(U_j^n) - f(U_{j-1}^n) \right) \quad (10)$$

with the notations from the previous section. If $f'(\cdot) < 0$ the upwind scheme is given by

$$U_j^{n+1} = U_j^n - \lambda \left(f(U_{j+1}^n) - f(U_j^n) \right). \quad (11)$$

The upwind scheme has a number of favourable stability properties. They can be summarised as follows:

Proposition 3.1 (Stability Properties of the Upwind Scheme)

Under the usual CFL stability condition², the upwind scheme is a local extremum diminishing (LED) scheme. It does not introduce new extrema during a computation, i.e., it diminishes also the number of extrema (NED property). Moreover, the upwind scheme satisfies a discrete maximum–minimum principle.

The proofs of the validity of the mentioned properties are simple, see for instance [6, 13] in the context of numerical schemes for conservation laws.

While the upwind scheme can also be shown to approximate the entropy solution³ of the underlying PDE, it has a severe disadvantage: it suffers from undesirable blurring effects aka *numerical viscosity*. To quantify these viscous artifacts we write the scheme (10) in its *viscosity form*, i.e.,

$$U_j^{n+1} = U_j^n - \frac{\lambda}{2} \left(f(U_{j+1}^n) - f(U_{j-1}^n) \right) \quad (12)$$

$$+ \frac{Q_{j+1/2}^n}{2} (U_{j+1}^n - U_j^n) - \frac{Q_{j-1/2}^n}{2} (U_j^n - U_{j-1}^n). \quad (13)$$

The basic idea behind this decomposition is to consider the part (12) of the method as a second-order approximation in space (and first order in time) of the underlying process, while part (13) is (in leading order) the discrete counterpart of the numerical diffusion incorporated in the scheme introduced by the spatial approximation.

One easily verifies that (10) and (12)–(13) can be made identical by choosing viscosity coefficients $Q_{j+1/2}^n$ and $Q_{j-1/2}^n$ that satisfy

$$Q_{j+1/2}^n = \lambda \frac{f_{j+1}^n - f_j^n}{U_{j+1}^n - U_j^n} \quad \text{and} \quad Q_{j-1/2}^n = \lambda \frac{f_j^n - f_{j-1}^n}{U_j^n - U_{j-1}^n} \quad (14)$$

²The Courant–Friedrichs–Lewy (CFL) condition is the fundamental stability criterion for numerical schemes for hyperbolic PDEs. It requires that the numerical domain of dependence is included in the analytical domain of dependence of the PDE [9, 19]. For the case of the upwind schemes (10) and (11) introduced above, the CFL condition reads $\Delta t \max |f'(U_j^n)|$, where the maximum is computed over the set $\{U_j^n\}$ of all given data.

³An entropy solution is a specific generalised solution, since classical, differentiable solutions are inappropriate to admit discontinuities that are characteristic for hyperbolic conservation laws.

for $U_{k+1}^n \neq U_k^n$, $k \in \{j, j-1\}$, and $f_i^l := f(U_i^l)$. By the prerequisite $f'(\cdot) \geq 0$ necessary to apply an upwinding in the fashion (10), it is ensured that the viscosities $Q_{j\pm 1/2}^n$ are nonnegative. The resulting numerical diffusion is responsible for undesirable blurring effects that are observed with this first-order method. Exactly the terms corresponding to (13), (14) will be negated in a suitable way during a subsequent, stabilised inverse diffusion step of the FCT routine.

Let us note that, although the viscosities $Q_{j\pm 1/2}^n$ in (14) are nonlinear for general f , we will see that in the case of dilation and erosion processes they are in fact simply constants determined by the chosen space-time mesh. Non-linear effects arise due to the required invariance under rotations as will be discussed in the section on the 2-D model.

3.2 The FCT Scheme for 1-D Dilation

We now derive the 1-D algorithm for dilation. The corresponding scheme for erosion can be constructed and discussed analogously.

3.2.1 The Formulation of the 1-D Upwind Basis Scheme

Let us define abbreviate notions for the *one-sided discrete differences*

$$\Delta U_{j+1/2}^k := U_{j+1}^k - U_j^k \quad (15)$$

and for the *centered discrete differences*

$$\Delta U_j^k := U_{j+1}^k - U_{j-1}^k. \quad (16)$$

In order to clarify the basic idea, let us point out explicitly, that a proper scheme describing the dilation process (5) satisfies the following

Principle 3.1 (Discrete Evolution Principle of the Dilation Process)

In order to reflect the properties of the analytical dilation operator, the following properties need to be satisfied on the discrete level:

- *In regions of (strictly) monotone data, the flow is directed from lower to higher grey values.*
- *Local minima are increased, while local maxima are maintained.*

For the development of our 1-D algorithm, it is useful to fix the attention to a particular spatial index j and to consider a diversion of cases with respect

to the data situations one may encounter.

Case I : $\Delta U_{j-1/2}^n \geq 0$ and $\Delta U_{j+1/2}^n > 0$.

For this case, the upwind scheme and its viscosity form read

$$\begin{aligned} U_j^{n+1} &= U_j^n + \lambda (U_{j+1}^n - U_j^n) \\ &= U_j^n + \underbrace{\frac{\lambda}{2} (U_{j+1}^n - U_{j-1}^n)}_{(a)} + \underbrace{\frac{\lambda}{2} (U_{j+1}^n - U_j^n) - \frac{\lambda}{2} (U_j^n - U_{j-1}^n)}_{(b)}. \end{aligned} \quad (17)$$

As indicated, (17)(a) is a second-order accurate approximation of $\Delta t |u_x|$, while (17)(b) implies $Q_{j\pm 1/2}^n = \lambda$ in the investigated case.

Case II : $\Delta U_{j-1/2}^n < 0$ and $\Delta U_{j+1/2}^n \leq 0$.

Here the upwind scheme and its viscosity form read

$$\begin{aligned} U_j^{n+1} &= U_j^n + \lambda (U_{j-1}^n - U_j^n) \\ &= U_j^n + \frac{\lambda}{2} (U_{j-1}^n - U_{j+1}^n) + \frac{\lambda}{2} (U_{j+1}^n - U_j^n) - \frac{\lambda}{2} (U_j^n - U_{j-1}^n), \end{aligned} \quad (18)$$

revealing the same structure as in (17), but the approximation of $\Delta t |u_x|$ is different here.

Case III : $\Delta U_{j-1/2}^n < 0$ and $\Delta U_{j+1/2}^n \geq 0$.

The investigated case especially incorporates the situation

$$\Delta U_{j-1/2}^n < 0 \quad \text{and} \quad \Delta U_{j+1/2}^n > 0,$$

i.e., a local minimum is located at the index j . Analogously to the proceeding within the Rouy–Tourin algorithm [25, 38], we choose the direction of the dilation flow according to the largest gradient, i.e.,

$$\begin{aligned} U_j^{n+1} &= U_j^n + \lambda \underbrace{\max(U_{j+1}^n - U_j^n, U_{j-1}^n - U_j^n)}_{:=\tilde{\Delta}U_j^n} \\ &= \begin{cases} U_j^n + \frac{\lambda}{2}\Delta U_j^n + \frac{\lambda}{2}\Delta U_{j+1/2}^n - \frac{\lambda}{2}\Delta U_{j-1/2}^n & \text{if } \tilde{\Delta}U_j^n = U_{j+1}^n - U_j^n, \\ U_j^n - \frac{\lambda}{2}\Delta U_j^n + \frac{\lambda}{2}\Delta U_{j+1/2}^n - \frac{\lambda}{2}\Delta U_{j-1/2}^n & \text{if } \tilde{\Delta}U_j^n = U_{j-1}^n - U_j^n. \end{cases} \end{aligned} \quad (19)$$

Note that this choice is not simply a matter of discrete modeling, it is also perfectly reasonable since

$$\pm \frac{\lambda}{2} \Delta U_j^n = \frac{\lambda}{2} (U_{j\pm 1}^n - U_{j\mp 1}^n) \approx \Delta t |u_x| \quad \text{for} \quad \tilde{\Delta}U_j^n = U_{j\pm 1}^n - U_j^n$$

is also a second-order accurate approximation of the dilation process at a local minimum of the data.

Case IV : $\Delta U_{j-1/2}^n \geq 0$ and $\Delta U_{j+1/2}^n \leq 0$.

Here, according to the formulated Principle 3.1, we set

$$U_j^{n+1} := U_j^n. \quad (20)$$

Summary of Cases I to IV : Having finished the consideration of all possible cases, we can formulate the upwind scheme as follows:

$$U_j^{n+1} = \begin{cases} U_j^n & \text{for } \Delta U_{j-1/2}^n \geq 0, \Delta U_{j+1/2}^n \leq 0, \\ U_j^n + \frac{\lambda}{2} |\Delta U_j^n| + \frac{\lambda}{2} \Delta U_{j+1/2}^n - \frac{\lambda}{2} \Delta U_{j-1/2}^n, & \text{else.} \end{cases} \quad (21)$$

The scheme (21) is, because of its treatment of local minima, identical with the 1-D version of the already mentioned Rouy–Tourin method, which is derived in a completely different fashion for the 2-D case. Thereby, for the 1-D case, the CFL stability condition reads $\Delta t \leq \Delta x$.

By the form (21) we have gained that we can identify the incorporated numerical viscosity arising by our approximation of the spatial derivative. Neglecting the influence of the first-order temporal approximation, we refer to the viscosity identified in the above fashion as the *numerical viscosity* of our scheme.

In order to illuminate the properties of the method (21), we apply it without further modification at a simple 1-D test problem depicted in Figure 2. We clearly observe the desired dilation process, however, the numerical solution is fairly blurry.

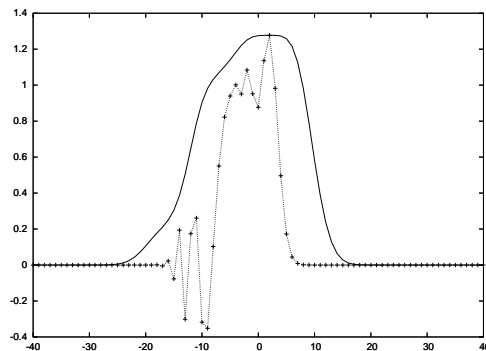


Figure 2: Oscillatory initial data and its dilation computed using the described first-order upwind scheme (21) ($\Delta x = 1$, $\Delta t = 0.2$, 30 iterations).

3.2.2 The 1-D FCT Step

Now we turn to the FCT methodology. For this, we use in the following the data notions:

- $U_j^{n+1/2}$ for the data obtained by the upwind scheme starting from U_j^n ,
- U_j^{n+1} for the data obtained after the inverse diffusion step.

When applying an inverse diffusion algorithm, it is evident that one has to incorporate a means of stabilisation. We would like to mention the

Principle 3.2 (of Boris and Book [3]) *No antidiffusive flux transfer of mass can push the density value at any grid point beyond the density value at neighboring points.*

The traditional FCT scheme realises this principle by computing antidiffusive fluxes $\tilde{g}_{j\pm 1/2}$, so that

$$U_j^{n+1} = U_j^{n+1/2} - \tilde{g}_{j+1/2} + \tilde{g}_{j-1/2} \quad (22)$$

follows. Thereby, Boris and Book use

$$\tilde{g}_{j+1/2} := \text{minmod} \left(\Delta U_{j-1/2}^{n+1/2}, \eta_{j+1/2} \Delta U_{j+1/2}^{n+1/2}, \Delta U_{j+3/2}^{n+1/2} \right), \quad (23)$$

$$\text{minmod}(a, b, c) := \text{sign}(b) \max \left(0, \min(\text{sign}(b)a, |b|, \text{sign}(b)c) \right), \quad (24)$$

where $\eta_{j+1/2}$ is obtained by an analysis of the *modified equation*, i.e., it is determined on the differential level; see especially [5].

In 1-D, our proceeding is similar. However, we negate as indicated the diffusion computed by the discrete *viscosity form* introduced before.

Thus, we realize Principle 3.2 ensuring the stability of the backward diffusion step by introducing stabilised inverse diffusion terms of type

$$g_{j+1/2} := \text{minmod} \left(\Delta U_{j-1/2}^{n+1/2}, \frac{\lambda}{2} \Delta U_{j+1/2}^{n+1/2}, \Delta U_{j+3/2}^{n+1/2} \right) \quad (25)$$

leading here, i.e., in 1-D, to the correction formula

$$U_j^{n+1} = U_j^{n+1/2} - g_{j+1/2} + g_{j-1/2}. \quad (26)$$

We can apply our FCT algorithm incorporating (i) the evolution step performed by the method (21) and (ii) the correction step (26) again at our 1-D test case. For the same computational parameters as before, we see in Figure 3 the initial data together with the solutions obtained using the upwind scheme and the new FCT scheme. Note the significantly sharper resolution obtained using the latter method while the location of fronts is captured correctly due to the properties of the underlying upwind scheme.

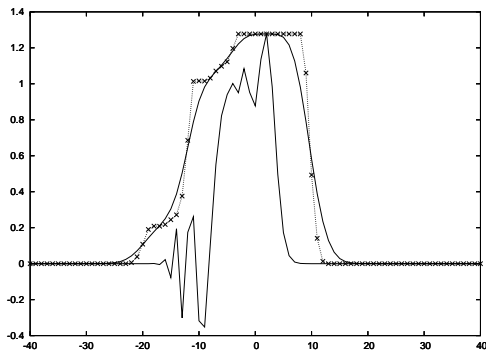


Figure 3: Oscillatory initial data together with the dilation process computed using (continuous line) the developed upwind scheme, and (dotted line) the new FCT scheme ($\Delta x = 1$, $\Delta t = 0.2$, 30 iterations).

3.2.3 Stability of the 1-D FCT scheme

In the context of morphological dilation processes, useful stability notions are a *global discrete maximum principle* as well as a *local discrete extremum principle*. We do not deal explicitly with minima since these are treated by the construction of the method in the usual fashion, increasing them. We proceed with the

Proposition 3.2 (Local Extremum Principle)

Let

$$\text{sign} \left(\Delta U_{k+1/2}^{n+1/2} \right) = \text{sign} \left(\Delta U_{k-1/2}^{n+1/2} \right) \neq 0 \quad (27)$$

hold. Then the FCT scheme defined by

$$U_j^{n+1} = U_j^{n+1/2} - g_{j+1/2} + g_{j-1/2} \quad (28)$$

using g from (25) satisfies locally a discrete maximum–minimum principle:

$$U_j^{n+1} \geq \min \left(U_{j-2}^n, U_{j-1}^n, U_j^n, U_{j+1}^n, U_{j+2}^n \right) \quad (29)$$

and

$$U_j^{n+1} \leq \max \left(U_{j-2}^n, U_{j-1}^n, U_j^n, U_{j+1}^n, U_{j+2}^n \right). \quad (30)$$

Proof. Since the upwind basic scheme satisfies a discrete maximum–minimum principle, it is sufficient to show the validity of

$$U_k^{n+1} \in \text{conv} \left(U_{k-1}^{n+1/2}, U_k^{n+1/2}, U_{k+1}^{n+1/2} \right)$$

where conv denotes the convex hull.

The crucial observation is, that for the assumption (27) the flux contributions

$$-g_{j+1/2} \quad \text{and} \quad +g_{j-1/2}$$

defined by (25) have opposite sign, i.e., even if, for instance, in the case $U_j^{n+1/2} > U_{j-1}^{n+1/2}$, we have within the estimation

$$U_j^{n+1/2} - g_{j+1/2} \geq U_j^{n+1/2} - \Delta U_{j-1/2}^{n+1/2} = U_j^{n+1/2} - \left(U_j^{n+1/2} - U_{j-1}^{n+1/2} \right) = U_{j-1}^{n+1/2}$$

in the worst case the validity of the exact equality

$$U_j^{n+1/2} - g_{j+1/2} = U_{j-1}^{n+1/2}.$$

In any case, the contribution due to $+g_{j-1/2}$ pushes the resulting value back into the interior of the convex hull of the values $U_j^{n+1/2}, U_{j-1}^{n+1/2}$:

$$\begin{aligned} U_j^{n+1} &= U_j^{n+1/2} - g_{j+1/2} + g_{j-1/2} \\ &\stackrel{\text{worst case}}{=} U_{j-1}^{n+1/2} + \underbrace{g_{j-1/2}}_{\geq 0} \\ &\in \text{conv}\left(U_{j-1}^{n+1/2}, U_j^{n+1/2}\right) \\ &\leq U_{j-1}^{n+1/2} + \frac{\lambda}{2} \left(U_j^{n+1/2} - U_{j-1}^{n+1/2} \right) \\ &= \left(1 - \frac{\lambda}{2} \right) U_{j-1}^{n+1/2} + \frac{\lambda}{2} U_j^{n+1/2}, \end{aligned}$$

imposing the stability condition $\lambda \leq 2$ which is satisfied for the upwind scheme anyway. The other possible cases can be treated analogously, concluding the proof. \blacksquare

Because of the properties of the minmod function, the core of the proof also works without the assumption (27). Thus we can give directly the desired

Corollary 3.1 (Global Maximum Principle)

The investigated scheme satisfies globally a discrete maximum principle.

As indicated, the erosion process can be investigated analogously, yielding a global discrete minimum principle and a local discrete extremum principle.

4 The Two-Dimensional FCT Algorithm

Let us now extend the one-dimensional analysis of the preceding section to the two-dimensional case. Also here, we only discuss the dilation process in detail.

4.1 The General Upwind Scheme in 2-D

The basis of the 2-D algorithm is a straightforward extension of the 1-D scheme. Since the underlying PDE reads as

$$\partial_t u = \|\nabla u\|_2 = \sqrt{|\partial_x u|^2 + |\partial_y u|^2}, \quad (31)$$

which, notably, incorporates an additive splitting of the terms constituted solely on u_x and u_y , respectively, we can simply employ the corresponding 1-D upwind expressions to obtain the basic 2-D upwind scheme for dilation processes with a disc.

In order to define this scheme, let us give the abbreviations

$$dU_i^n := \frac{\lambda}{2} |U_{i+1,j}^n - U_{i-1,j}^n| + \frac{\lambda}{2} (U_{i+1,j}^n - U_{ij}^n) - \frac{\lambda}{2} (U_{ij}^n - U_{i-1,j}^n), \quad (32)$$

$$dU_j^n := \frac{\lambda}{2} |U_{i,j+1}^n - U_{i,j-1}^n| + \frac{\lambda}{2} (U_{i,j+1}^n - U_{ij}^n) - \frac{\lambda}{2} (U_{ij}^n - U_{i,j-1}^n), \quad (33)$$

$$\Delta U_{i,j+1/2}^k := U_{i,j+1}^k - U_{ij}^k \quad \text{and} \quad \Delta U_{i+1/2,j}^k := U_{i+1,j}^k - U_{ij}^k. \quad (34)$$

Then the scheme reads

$$U_{ij}^{n+1} = \begin{cases} U_{ij}^n & \text{for } \Delta U_{i-1/2,j}^n, \Delta U_{i,j-1/2}^n \geq 0 \text{ and } \Delta U_{i+1/2,j}^n, \Delta U_{i,j+1/2}^n \leq 0, \\ U_{ij}^n + \sqrt{(dU_i^n)^2 + (dU_j^n)^2} & \text{else.} \end{cases} \quad (35)$$

For the scheme (35) again Proposition 3.1 holds, ensuring reasonable properties of the method.

As in the 1-D case, one can apply the method (35) without further modification, compare Figure 1. However, as already indicated, any numerical solution is fairly blurred at the edges incorporated in an image. Note, that the rotational invariance of the scheme (35) is obvious due to the consideration of the 2-norm.

For the application of a FCT strategy, it is crucial to observe that *there is no general way to extract the discrete viscosity terms out of the square root in (35)*. This is exactly the reason why we have to go a different way which

distinguishes our scheme from other FCT schemes in the multidimensional setting. Note also, that we can now understand that our proceeding in the 1-D case has the character of the treatment of a special case: in 1-D, the $\partial_y u$ -type terms in (35) can be omitted, so that finally – after taking $\sqrt{(\cdot)^2}$ – the discrete viscosity terms can be separated directly in an additive fashion from the second-order discretisation of $|\partial_x u|$.

4.2 The FCT formulation

We proceed in treating the non-maximum case of (35), i.e.,

$$U_{ij}^{n+1} = U_{ij}^n + \sqrt{(dU_i^n)^2 + (dU_j^n)^2}, \quad (36)$$

in order to derive our 2-D FCT scheme for dilation.

Essential for the definition of our FCT procedure is to split a *viscous part* from a *second-order part*. Thus, we add zero in (36) obtaining

$$\begin{aligned} U_{ij}^{n+1} &= U_{ij}^n + \sqrt{(dU_i^n)^2 + (dU_j^n)^2} \\ &\quad + \sqrt{\left(\frac{\lambda}{2} |U_{i+1,j}^n - U_{i-1,j}^n|\right)^2 + \left(\frac{\lambda}{2} |U_{i,j+1}^n - U_{i,j-1}^n|\right)^2} \\ &\quad - \sqrt{\left(\frac{\lambda}{2} |U_{i+1,j}^n - U_{i-1,j}^n|\right)^2 + \left(\frac{\lambda}{2} |U_{i,j+1}^n - U_{i,j-1}^n|\right)^2}. \end{aligned} \quad (37)$$

Consequently, we now identify the viscous part as

$$-\sqrt{\left(\frac{\lambda}{2} |U_{i+1,j}^n - U_{i-1,j}^n|\right)^2 + \left(\frac{\lambda}{2} |U_{i,j+1}^n - U_{i,j-1}^n|\right)^2} + \sqrt{(dU_i^n)^2 + (dU_j^n)^2},$$

while

$$U_{ij}^{n+1} = U_{ij}^n + \sqrt{\left(\frac{\lambda}{2} |U_{i+1,j}^n - U_{i-1,j}^n|\right)^2 + \left(\frac{\lambda}{2} |U_{i,j+1}^n - U_{i,j-1}^n|\right)^2}$$

defines the separated (spatial) second-order part.

Note that the viscous part is now nonlinear and it cannot be split up additively further into viscous fluxes due to the dimensional influence. For the FCT procedure, it must be handled as one block.

Analogously to (32), (33), we now introduce the abbreviations

$$g_{i+1/2,j} := \text{minmod} \left(\Delta U_{i-1/2,j}^{n+1/2}, \frac{\lambda}{2} \Delta U_{i+1/2,j}^{n+1/2}, \Delta U_{i+3/2,j}^{n+1/2} \right), \quad (38)$$

$$g_{i,j+1/2} := \text{minmod} \left(\Delta U_{i,j-1/2}^{n+1/2}, \frac{\lambda}{2} \Delta U_{i,j+1/2}^{n+1/2}, \Delta U_{i,j+3/2}^{n+1/2} \right). \quad (39)$$

Following then consequently the FCT strategy, we define

$$Q_h^{n+1/2} := \sqrt{\left(\frac{\lambda}{2} \left| U_{i+1,j}^{n+1/2} - U_{i-1,j}^{n+1/2} \right| \right)^2 + \left(\frac{\lambda}{2} \left| U_{i,j+1}^{n+1/2} - U_{i,j-1}^{n+1/2} \right| \right)^2}, \quad (40)$$

$$Q_l^{n+1/2} := \sqrt{\left(\delta U_i^{n+1/2} \right)^2 + \left(\delta U_j^{n+1/2} \right)^2}, \quad (41)$$

where the *stabilised backward diffusive fluxes* are incorporated by

$$\delta U_i^{n+1/2} := \frac{\lambda}{2} \left| U_{i+1,j}^{n+1/2} - U_{i-1,j}^{n+1/2} \right| + g_{i+1/2,j} - g_{i-1/2,j}, \quad (42)$$

$$\delta U_j^{n+1/2} := \frac{\lambda}{2} \left| U_{i,j+1}^{n+1/2} - U_{i,j-1}^{n+1/2} \right| + g_{i,j+1/2} - g_{i,j-1/2}, \quad (43)$$

and we correct the 2-D viscous basis scheme (35) by

$$U_{ij}^{n+1} = U_{ij}^{n+1/2} + Q_h^{n+1/2} - Q_l^{n+1/2} \quad (44)$$

using a notation analogously to the one in the preceding section.

We test our new FCT dilation scheme by considering again the dilation of a disc; see Figure 4 for a comparison with the first-order upwind scheme. We see that a significantly sharper resolution of the evolving circle boundaries is obtained.

In a second experiment, we consider the real-world test image from Figure 5. Also in this case the FCT dilation algorithm gives the desired sharp resolution.

4.3 Stability in 2-D

We now investigate the crucial stability properties of the method, meaning the validity of a *local extremum principle* and a *global discrete maximum principle*, respectively. As indicated, the major difficulty in the 2-D case is imposed by the nonlinearities due to the dimensional influence in (40)-(43).

Theorem 4.1 (Local Extremum Principle) *The described FCT dilation scheme (44) satisfies locally a discrete maximum–minimum principle.*

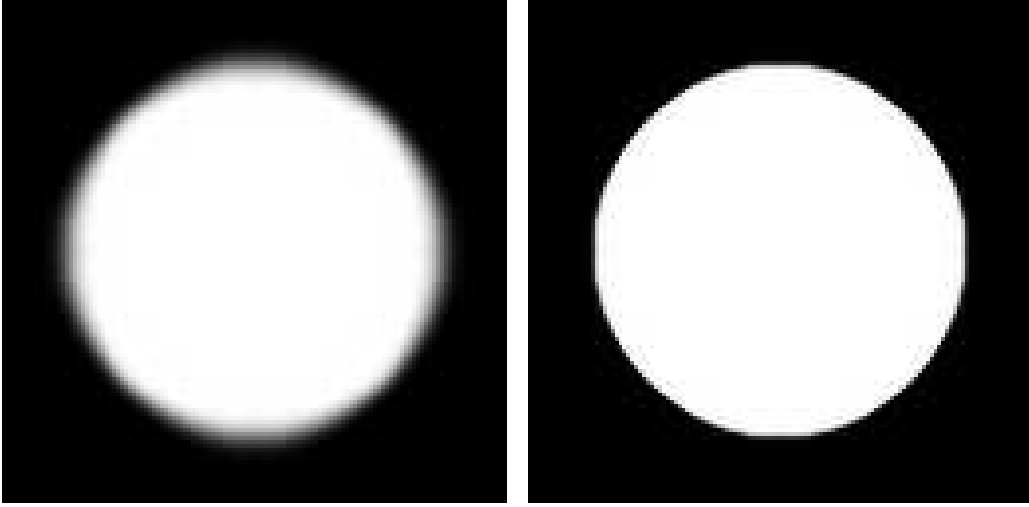


Figure 4: **(a) Left:** Dilation of Figure 1(a), computed by the first-order upwind scheme ($\Delta x = \Delta y = 1$, $\Delta t = 0.5$, 30 iterations). **(b) Right:** Computed by our new FCT scheme (same parameters).



Figure 5: **(a) Left:** Initial image, 256×256 pixels. **(b) Right:** Dilation computed by our new FCT scheme ($\Delta x = \Delta y = 1$, $\Delta t = 0.5$, 30 iterations).

Proof. It is useful to introduce the abbreviations

$$\alpha_i := \frac{\lambda}{2} \left| U_{i+1,j}^{n+1/2} - U_{i-1,j}^{n+1/2} \right|, \quad \alpha_j := \frac{\lambda}{2} \left| U_{i,j+1}^{n+1/2} - U_{i,j-1}^{n+1/2} \right|, \quad (45)$$

$$\beta_i := g_{i+1/2,j} - g_{i-1/2,j}, \quad \beta_j := g_{i,j+1/2} - g_{i,j-1/2}, \quad (46)$$

for defining the vectors

$$\vec{\alpha} := (\alpha_i, \alpha_j)^T \quad \text{and} \quad \vec{\beta} := (\beta_i, \beta_j)^T. \quad (47)$$

Using (45)-(47), we can rewrite $Q_h^{n+1/2}$ and $Q_l^{n+1/2}$ from (40) and (41) as:

$$Q_h^{n+1/2} = \|\vec{\alpha}\|_2, \quad Q_l^{n+1/2} = \|\vec{\alpha} + \vec{\beta}\|_2, \quad (48)$$

and the updated formula (44) reads

$$U_{ij}^{n+1} = U_{ij}^{n+1/2} + \|\vec{\alpha}\|_2 - \|\vec{\alpha} + \vec{\beta}\|_2. \quad (49)$$

Concerning a further analysis of (49), let us point out that we have on the one hand

$$\begin{aligned} \|\vec{\alpha}\|_2 - \|\vec{\alpha} + \vec{\beta}\|_2 &= \|\vec{\alpha} + \vec{\beta} - \vec{\beta}\|_2 - \|\vec{\alpha} + \vec{\beta}\|_2 \\ &\leq \|\vec{\alpha} + \vec{\beta}\|_2 + \|\vec{\beta}\|_2 - \|\vec{\alpha} + \vec{\beta}\|_2 \\ &= \|\vec{\beta}\|_2, \end{aligned} \quad (50)$$

while we can also easily deduce

$$\|\vec{\alpha}\|_2 - \|\vec{\alpha} + \vec{\beta}\|_2 \geq \|\vec{\alpha}\|_2 - (\|\vec{\alpha}\|_2 + \|\vec{\beta}\|_2) = -\|\vec{\beta}\|_2. \quad (51)$$

Assembling (50) and (51), we obtain

$$|\|\vec{\alpha}\|_2 - \|\vec{\alpha} + \vec{\beta}\|_2| \leq \|\vec{\beta}\|_2. \quad (52)$$

For convenience, let us for the moment assume that

$$\text{sign} \left(\Delta U_{i+1/2,j}^{n+1/2} \right) = \text{sign} \left(\Delta U_{i-1/2,j}^{n+1/2} \right) \neq 0, \quad (53)$$

$$\text{sign} \left(\Delta U_{i,j+1/2}^{n+1/2} \right) = \text{sign} \left(\Delta U_{i,j-1/2}^{n+1/2} \right) \neq 0 \quad (54)$$

hold. Furthermore, let us consider local data maxima

$$U_{i+1,j}^{n+1/2} > U_{ij}^{n+1/2} > U_{i-1,j}^{n+1/2} \quad \text{and} \quad U_{i,j+1}^{n+1/2} > U_{ij}^{n+1/2} > U_{i,j-1}^{n+1/2}. \quad (55)$$

By the construction of the flux function g , see (38) and (39), we can transfer directly the argument of the proof of Lemma 3.2 in order to see that $\|\vec{\beta}\|_2$ is limited by

$$\frac{\lambda}{2} \sqrt{\left(U_{i+1,j}^{n+1/2} - U_{ij}^{n+1/2} \right)^2 + \left(U_{i,j+1}^{n+1/2} - U_{ij}^{n+1/2} \right)^2}. \quad (56)$$

Taking the maximum out of the differences $\Delta U_{i+1/2,j}^{n+1/2}$ and $\Delta U_{i,j+1/2}^{n+1/2}$ occurring in (56), it follows that the antidiffusive flux contributions can be estimated via

$$\frac{\lambda}{2}\sqrt{2}\max\left(U_{i+1,j}^{n+1/2}-U_{ij}^{n+1/2}, U_{i,j+1}^{n+1/2}-U_{ij}^{n+1/2}\right), \quad (57)$$

i.e., we obtain the validity of a local discrete maximum principle under the condition

$$\frac{\lambda}{2}\sqrt{2}\leq 1 \quad \Leftrightarrow \quad \lambda\leq\sqrt{2}$$

which is satisfied anyway by the CFL condition of the upwind scheme which reads in 2-D as $\lambda\leq 1/\sqrt{2}$. ■

Remarks

- (a) Let us note that, by construction, the proof of Theorem 4.1 can easily be extended to higher dimensions.
- (b) By our derivation of the algorithm and by the proof of Theorem 4.1, it is clear that the crucial restriction imposed on the time step size is due to the CFL condition for the upwind scheme, and not due to the antidiffusion step.
- (c) The above procedure can easily be employed analogously for the erosion process; see Figure 6 for computations using the resulting 2-D FCT erosion scheme. Thus, for both dilation and erosion we obtain a discrete maximum–minimum principle as well as a global extremum principle, respectively.

5 Summary and Conclusions

We have presented a novel FCT type algorithm for morphological dilation and erosion processes with a disc as structuring element. It features the desirable properties of *rotational invariance* and *sharp resolution*. Moreover, the algorithm can easily be extended to a higher-dimensional setting while retaining these qualities. Technically, we have employed an unconventional nonlinear genuinely multidimensional formulation of antidiffusive fluxes in order to achieve these goals. The resolution of the new method outperforms the Rouy-Tourin and Osher-Sethian schemes that are frequently used in PDE-based mathematical morphology. Compared to other FCT approaches the scheme is competitive, while we rely on the discretisation of the underlying



Figure 6: **(a) Left:** Eroded disc using Figure 1 (a) as initial image and our FCT scheme with $\Delta x = \Delta y = 1$, $\Delta t = 0.5$, and 30 iterations. **(b) Right:** Erosion process with our FCT scheme applied to the Figure 5 (a) as initial image, here with $\Delta x = \Delta y = 1$, $\Delta t = 0.5$, and 10 iterations.

PDE. Our work has addressed the main shortcoming of PDE-based morphological algorithms and makes their resolution at shock fronts comparable to set-based morphological schemes.

In our ongoing research we study extensions of this FCT approach to morphological PDEs with other non-digitally scalable structuring elements such as ellipses.

Acknowledgements. The authors gratefully acknowledge the financial support of their work by the *Deutsche Forschungsgemeinschaft (DFG)* under the grants SO 363/9-1 and WE 2602/1-2.

References

- [1] L. Alvarez, F. Guichard, P.-L. Lions, and J.-M. Morel. Axioms and fundamental equations in image processing. *Archive for Rational Mechanics and Analysis*, 123:199–257, 1993.
- [2] A. B. Arehart, L. Vincent, and B. B. Kimia. Mathematical morphology: The Hamilton–Jacobi connection. In *Proc. Fourth International Conference on Computer Vision*, pages 215–219, Berlin, May 1993. IEEE Computer Society Press.

- [3] J. P. Boris and D. L. Book. Flux corrected transport. I. SHASTA, a fluid transport algorithm that works. *Journal of Computational Physics*, 11(1):38–69, 1973.
- [4] J. P. Boris and D. L. Book. Flux corrected transport. III. Minimal error FCT algorithms. *Journal of Computational Physics*, 20:397–431, 1976.
- [5] J. P. Boris, D. L. Book, and K. Hain. Flux corrected transport. II. Generalizations of the method. *Journal of Computational Physics*, 18:248–283, 1975.
- [6] M. Breuß, T. Brox, T. Sonar, and J. Weickert. Stabilized nonlinear inverse diffusion for approximating hyperbolic PDEs. In R. Kimmel, N. Sochen, and J. Weickert, editors, *Scale-Space and PDE Methods in Computer Vision*, volume 3459 of *Lecture Notes in Computer Science*, pages 536–547, Berlin, 2005. Springer.
- [7] R. W. Brockett and P. Maragos. Evolution equations for continuous-scale morphology. In *Proc. IEEE International Conference on Acoustics, Speech and Signal Processing*, volume 3, pages 125–128, San Francisco, CA, Mar. 1992.
- [8] M. A. Butt and P. Maragos. Comparison of multiscale morphology approaches: PDE implemented via curve evolution versus Chamfer distance transform. In P. Maragos, R. W. Schafer, and M. A. Butt, editors, *Mathematical Morphology and its Applications to Image and Signal Processing*, volume 5 of *Computational Imaging and Vision*, pages 31–40. Kluwer, Dordrecht, 1996.
- [9] R. Courant, K. Friedrichs, and H. Lewy. Über die partiellen Differenzgleichungen der mathematischen Physik. *Mathematische Annalen*, 100:32–74, 1928.
- [10] E. R. Dougherty. *Mathematical Morphology in Image Processing*. Marcel Dekker, New York, 1993.
- [11] L. C. Evans. *Partial Differential Equations*, volume 19 of *Graduate Studies in Mathematics*. American Mathematical Society, Providence, 1998.
- [12] S. J. Farlow. *Partial Differential Equations for Scientists and Engineers*. Dover, New York, 1993.

- [13] E. Godlewski and P.-A. Raviart. *Hyperbolic Systems of Conservation Laws*. Edition Marketing, 1991.
- [14] J. Goutsias, L. Vincent, and D. S. Bloomberg, editors. *Mathematical Morphology and its Applications to Image and Signal Processing*, volume 18 of *Computational Imaging and Vision*. Kluwer, Dordrecht, 2000.
- [15] H. J. A. M. Heijmans. *Morphological Image Operators*. Academic Press, Boston, 1994.
- [16] H. J. A. M. Heijmans and J. B. T. M. Roerdink, editors. *Mathematical Morphology and its Applications to Image and Signal Processing*, volume 12 of *Computational Imaging and Vision*. Kluwer, Dordrecht, 1998.
- [17] D. Kuzmin, R. Löhner, and S. Turek, editors. *Flux-Corrected Transport*. Springer, Berlin, 2005.
- [18] D. Kuzmin and S. Turek. Flux correction tools for finite elements. *Journal of Computational Physics*, 175:525–558, 2002.
- [19] R. J. LeVeque. *Finite Volume Methods for Hyperbolic Problems*. Cambridge University Press, Cambridge, UK, 2002.
- [20] P. Maragos, R. W. Schafer, and M. A. Butt, editors. *Mathematical Morphology and its Applications to Image and Signal Processing*, volume 5 of *Computational Imaging and Vision*. Kluwer, Dordrecht, 1996.
- [21] G. Matheron. *Random Sets and Integral Geometry*. Wiley, New York, 1975.
- [22] S. Osher and R. P. Fedkiw. *Level Set Methods and Dynamic Implicit Surfaces*, volume 153 of *Applied Mathematical Sciences*. Springer, New York, 2002.
- [23] S. Osher and J. A. Sethian. Fronts propagating with curvature-dependent speed: Algorithms based on Hamilton–Jacobi formulations. *Journal of Computational Physics*, 79:12–49, 1988.
- [24] C. Ronse, L. Najman, and E. Decencière, editors. *Mathematical Morphology: 40 Years On*, volume 30 of *Computational Imaging and Vision*. Springer, Dordrecht, 2005.
- [25] E. Rouy and A. Tourin. A viscosity solutions approach to shape-from-shading. *SIAM Journal on Numerical Analysis*, 29:867–884, 1992.

- [26] G. Sapiro, R. Kimmel, D. Shaked, B. B. Kimia, and A. M. Bruckstein. Implementing continuous-scale morphology via curve evolution. *Pattern Recognition*, 26:1363–1372, 1993.
- [27] M. Schmitt and J. Mattioli. *Morphologie mathématique*. Masson, Paris, 1993.
- [28] J. Serra. *Image Analysis and Mathematical Morphology*, volume 1. Academic Press, London, 1982.
- [29] J. Serra. *Image Analysis and Mathematical Morphology*, volume 2. Academic Press, London, 1988.
- [30] J. Serra and P. Salembier, editors. *Proc. International Workshop on Mathematical Morphology and its Applications to Signal Processing*. Barcelona, Spain, May 1993.
- [31] J. Serra and P. Soille, editors. *Mathematical Morphology and its Applications to Image Processing*, volume 2 of *Computational Imaging and Vision*. Kluwer, Dordrecht, 1994.
- [32] J. A. Sethian. *Level Set Methods and Fast Marching Methods*. Cambridge University Press, Cambridge, UK, second edition, 1999. Paperback edition.
- [33] K. Siddiqi, B. B. Kimia, and C.-W. Shu. Geometric shock-capturing ENO schemes for subpixel interpolation, computation and curve evolution. *Graphical Models and Image Processing*, 59:278–301, 1997.
- [34] P. Soille. *Morphological Image Analysis*. Springer, Berlin, second edition, 2003.
- [35] P. Stoll, C. Shu, and B. B. Kimia. Shock-capturing numerical methods for viscosity solutions of certain PDEs in computer vision: The Godunov, Osher–Sethian and ENO schemes. Technical Report LEMS-132, Division of Engineering, Brown University, Providence, RI, 1994.
- [36] H. Talbot and R. Beare, editors. *Proc. Sixth International Symposium on Mathematical Morphology and its Applications*. Sydney, Australia, April 2002. <http://www.cmis.csiro.au/ismm2002/proceedings/>.
- [37] R. van den Boomgaard. *Mathematical Morphology: Extensions Towards Computer Vision*. PhD thesis, University of Amsterdam, The Netherlands, 1992.

- [38] R. van den Boomgaard. Numerical solution schemes for continuous-scale morphology. In M. Nielsen, P. Johansen, O. F. Olsen, and J. Weickert, editors, *Scale-Space Theories in Computer Vision*, volume 1682 of *Lecture Notes in Computer Science*, pages 199–210. Springer, Berlin, 1999.
- [39] S. T. Zalesak. Fully multidimensional flux-corrected transport algorithms for fluids. *Journal of Computational Physics*, 31:335–362, 1979.
- [40] S. T. Zalesak. Introduction to "Flux corrected transport. I. SHASTA, a fluid transport algorithm that works". *Journal of Computational Physics*, 135:170–171, 1997.

Appendix

For the convenience of the interested reader, we give a brief compilation of the 2-D dilation/erosion algorithms.

The Dilation Algorithm

- (I) Predictor step with Upwind scheme.
Compute $U^{n+1/2}$ from U^n according to (35) with $\Delta t \leq 1/\sqrt{2}$.
- (II) Corrector step with stabilised inverse diffusion scheme.
Compute U^{k+1} from $U^{k+1/2}$ by (44), thereby assembling the ingredients (38), (39), (42), (43) within (40) and (41).

The Erosion Algorithm

- (I) Predictor step with Upwind scheme, using instead of (35) but by the same stability condition as for the dilation scheme:

$$U_{ij}^{n+1} = \begin{cases} U_{ij}^n & \text{for } \Delta U_{i-1/2,j}^n, \Delta U_{i,j-1/2}^n \leq 0 \\ & \text{and } \Delta U_{i+1/2,j}^n, \Delta U_{i,j+1/2}^n \geq 0, \\ U_{ij}^n - \sqrt{(dU_i^n)^2 + (dU_j^n)^2}, & \text{else,} \end{cases}$$

where

$$\begin{aligned} dU_i^n &:= \frac{\lambda}{2} |U_{i+1,j}^n - U_{i-1,j}^n| - \frac{\lambda}{2} (U_{i+1,j}^n - U_{ij}^n) + \frac{\lambda}{2} (U_{ij}^n - U_{i-1,j}^n), \\ dU_j^n &:= \frac{\lambda}{2} |U_{i,j+1}^n - U_{i,j-1}^n| - \frac{\lambda}{2} (U_{i,j+1}^n - U_{ij}^n) + \frac{\lambda}{2} (U_{ij}^n - U_{i,j-1}^n). \end{aligned}$$

- (II) Corrector step with stabilised inverse diffusion scheme.
Compute U^{k+1} from $U^{k+1/2}$ by (44), using the definitions

$$\begin{aligned} Q_h^{n+1/2} &:= -\sqrt{\left(\frac{\lambda}{2} |U_{i+1,j}^{n+1/2} - U_{i-1,j}^{n+1/2}|\right)^2 + \left(\frac{\lambda}{2} |U_{i,j+1}^{n+1/2} - U_{i,j-1}^{n+1/2}|\right)^2}, \\ Q_l^{n+1/2} &:= -\sqrt{(\delta U_i^{n+1/2})^2 + (\delta U_j^{n+1/2})^2}, \end{aligned}$$

with

$$\begin{aligned} \delta U_i^{n+1/2} &:= \frac{\lambda}{2} |U_{i+1,j}^{n+1/2} - U_{i-1,j}^{n+1/2}| - g_{i+1/2,j} + g_{i-1/2,j}, \\ \delta U_j^{n+1/2} &:= \frac{\lambda}{2} |U_{i,j+1}^{n+1/2} - U_{i,j-1}^{n+1/2}| - g_{i,j+1/2} + g_{i,j-1/2}. \end{aligned}$$